Pore Size Distribution and Microstructure of Oil Palm Shell Heat Treated at 300ºC Followed by Slow- or Fast Heating Treatment

Joko Sulistyo, Toshimitsu Hata, Yuji Imamura, Purnomo Darmadji, and Sri Nugroho Marsoem

Abstract

Pore size distribution and microstructure development of oil palm shell heat treated at 300ºC and treated at 300ºC and recarbonization at 600ºC followed by slow- or fast heating treatment up to 700ºC were investigated by small angle X-ray scattering (SAXS), N_2 gas adsorption and Raman spectroscopy. On oil palm shell heat-treated at 300ºC, slow heating treatment gave the widening micropore along with the ordering microstructure; but fast heating treatment produced charcoal with a narrow diameter of micropore with wider pore size distribution and the disordering microstructure. On oil palm shell heat treated at 300ºC and recarbonization at 600ºC, slow heating treatment contributed on the opening new micropore with ordering microstructure, but some parts of micropore showing inaccessible for N_2 gas. Meanwhile, fast heating treatment with the heating rate from 75 to 250ºC/min increased BET surface area with similar pore size distribution and the disordering microstructure.

Keywords: Oil palm shell charcoal, pore size distribution, microstructure, slow- fast heating treatment, SAXS, Raman spectroscopy.

Introduction

Charcoal is carbonaceous material produced from carbonization process of biomass including wood and other biomass such as oil palm shell. The microstructure of charcoal consists of porosity which is the gaps between elementary graphitic crystallites and carbon skeleton which is formed by a graphitic sheet with a random orientation. The microstructure of charcoal from biomass is considered to provide an important contribution for the control in the development of biomass carbon based material (Ishimaru *et al.* 2007). In recent years, the microstructure of biomass based carbon has been used as the template for the formation of SiC, SiC/C and SiC/SiO_2/C composites (Greil 2001; Fujisawa *et al*. 2004; Vyshnyakova *et al*. 2006; Sulistyo *et al*. 2010). A detailed microstructural study of softwood pyrolysis performed by Paris *et al.* (2005) showed that the charring process commenced with the formation and growth of aromatic structures and nanopores at temperature higher than 327ºC. The ordering of the carbon structures occurred with the increase of heat treatment temperature from 400-800ºC (Yamauchi and Kurimoto 2003). This report had a good agreement with previous studies which defined that the formation microporosity system at 500ºC and used of the temperature range in the preparation of charcoal for activated carbons (Mackay and Roberts 1981; Pastor-Villegas *et al*. 1993; Lua *et al*. 2006). Carbonization at a temperature of 700ºC was conducted to prepare the charcoal for porous SiC ceramic (Fujisawa *et al*. 2004). Therefore, a condition of the carbonization especially temperature, obviously very much influence charcoal with the proper microstructure for production of carbon based materials.

Charcoal with a low degree of order of microstructure is generated from the production of smoke liquid from oil palm shell. The smoke liquid production is run at low temperature heat treatment of 300ºC to maximize the yield of liquid product and to minimize the content of polyaromatic hydrocarbons (Hattula *et al*. 2001; Demirbas 2001). A large amount of this solid waste charcoal material with high carbon content is potentially used as precursors for the preparation of adsorbents and for lignocellulosic ceramics such as SiC composites. However, the microstructure in the charcoal limits the further application and utilization. Until now, fewer studies have been reported on the utilization of the charcoal heat-treated at 300ºC.

Heat treatment of the solid waste charcoal oil palm shell was necessary to be carried out to improve a degree of the order of the microstructure in the material. The heat treatment of rockrose wood with a heating rate of 10ºC/min develops the charcoal with pores in the range of micro- to macropores (Pastor-Villegas *et al*. 1993). Heat treatment at a slow heating rate up to 800ºC removes volatile matters with a series of chemical reactions such as dehydration, breaking the C-O, C=O and C-C bonds, or repolymerization (Kurosaki *et al*. 2007). On the other hand, the fast heating with the rate of 6000ºC/min up to 800ºC made the chemical reactions occur concurrently and produced the charcoal with macroporous structure. In this study, the heat treatments with large different heating rates were carried out in order to produce the charcoal with different pore structures and microstructures from oil palm shell heat-treated at 300ºC. The pore size distribution and microstructure of oil palm shell heat-treated at 300ºC followed by slow-or fast heating treatments up to 700ºC were investigated by small angle X-ray scattering (SAXS) and Raman spectroscopy. The

effect of reaction times in slow heating treatment and that of heating rates in fast heating treatment were examined in this study.

Experimental

Heat Treatment

Air dried oil palm shell (OPS) with the characteristics as shown in Table 1 was heat-treated at a rate of 10ºC/min and was maintained constant at 300ºC for 180 min in an electric cylindrical steel furnace of 1 kg capacity. The charcoal heat-treated at 300ºC noted as HT1. The furnace was connected to a water-cooled condenser to entrap liquid by cooling smoke. After heat treatment, HT1 charcoals were granulated by a hammer mill to be sieved to 63-150 µm. As the comparison of the effect of heating at 600ºC, part of HT1 samples were re-carbonized up to 600ºC at 10ºC/min and were then held at this temperature for 60 min in a muffle furnace. The charcoal from the heat treatment at 300ºC and then followed by re-carbonization at 600ºC noted as HT2.

Slow Heating Treatment

Dry weight of 20 g of HT1 or HT2 charcoal was mixed with 40 ml distilled water containing 4 g of $ZnCl_2$ at 60ºC. The small amount of $ZnCl_2$ was used in the mixture to aid in porosity development in charcoal (Rodriguez-Reinoso and Molina-Sabio 1992). The dehydrated materials were dried at 115ºC for 3 h in an electric oven and then were heat-treated at 10 °C/min up to 700ºC, and then kept for 60, 120 and 180 min in a muffle furnace. After cooling, charcoals were washed with 0.1 N HCl and water and then were dried at 115ºC.

Fast Heating Treatment

Dry weight of 0.2 g of HT1 or HT2 charcoal was put into a 10 mm of the diameter of graphite die with a length of 5 cm (point 1 in Fig. 1) which was closed with two graphite punches (point 2 in Fig. 1) with a length of 2.5 and 2.2 cm. The charcoal in the graphite die was placed in a pulse current sintering apparatus (VCSP-II, SS-Alloy Co. Ltd., Hiroshima) as sketched in Fig. 1. The charcoal was heat-treated at 75, 250, 1000 and 2000ºC/min up to 700ºC and was kept for 15 min under N_2 gas flow with a rate of 100 mL/min. A pressure of 12 MPa on the graphite die which had minimum effects on the charcoal was applied from the start of the heating and was released after cooling.

Tabel 1. Proximate and ultimate analysis of raw and carbonized material oil palm shell.

Samples	Proximate and ultimate analysis (%, dry basis)						
	Volatile matter	Fixed carbon	Ash	C	H	N	$O_{diff.}$
OPS	73.08	13.30	2.37	49.64	6.76	0.20	41.03
HT1	22.31	36.52	5.69	77.95	2.05	0.22	14.09
HT2	10.81	69.73	6.45	89.39	2.44	0.16	1.56

Note: OPS is raw oil palm shell. HT1 charcoal is oil palm shell heat-treated at 300ºC for 180 min; HT2 charcoal is oil palm shell heat-treated at 300ºC for 180 min and then followed by re-carbonization at 600ºC for 60 min. $O_{diff.}$ is estimated by difference from 100-C-H-N- Ash elements.

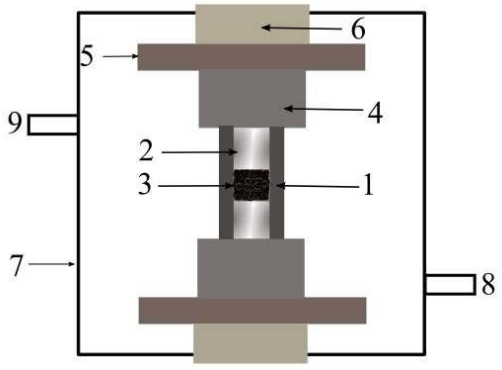

Figure 1. Schematic of a pulse current sintering apparatus. (1) Graphite die; (2) graphite punch; (3) sample; (4) graphite disc; (5) graphite plate; (6) copper electrode; (7) chamber; (8) vacuum pump; and (9) optical pyrometer.

Pore Distribution, Surface Area, and Microstructure Analysis

The pore size and distribution were analyzed by a three-slit optical systems with a line focus of SAXS (small-angle X-ray scattering, Rigaku Corporation, Japan). X-ray generator was operated at 50 kV and 200 mA. The intensity was measured with a scintillation counter. The scattered intensity was recorded as a function of the scattering wave vector,

$$q = \frac{4\pi}{\lambda}\sin\frac{\theta}{2} \quad (1)$$

where λ is the X-ray wavelength and 2θ is the scattering angle. The scattered intensity of charcoal which was put into a transparent capiller (Borokapillaren glas, Germany) with a diameter of 1 mm and a length of 80 mm was corrected by that of the transparent capiller without charcoal.

The pore size distribution was analyzed by using NANO-Solver Ver. 3.4 (Rigaku Corporation, Japan). This software program conducted profile fittings over the entire measurement range of scattered intensity in order to improve reproducibility in analysis. Least-squares methods were adopted to optimize the fitting parameters for a spherical model, assuming dispersed spheres. The spherical model which was fitted to the measurement data calculated the scattering intensity which depended on the form factor and structure factor using the following equation (Rigaku Corporation 2006):

$$I(q) = |F(q)|^2 S(q) \quad (2)$$

where *F(q)* is the form factor of the pore with a sphere shape possessing a radius R, and *S(q)* is the structure factor which is equal 1 when the pores are randomly distributed in the medium. The spherical model with a radius of R is used in the description of form factor (Rigaku Corporation 2006) as follow

$$F(q, D) = \Delta\rho \frac{4\pi}{q^3}\left(\sin(qR) - qR\cos(qr)\right) \quad (3)$$

where $\Delta\rho$ is electron density difference at position R. The structure factors are expressed by following equations (Rigaku Corporation 2006):

$$S(q) = 1 + \int_v \left(n(r) - n_0\right) e^{iq.r}\, dr \quad (4)$$

where n_0 is average particle density. The pore distribution assumes Γ distributions which are expressed by the following equation (Rigaku Corporation 2006)

$$P_{R_0}^M(R) = \frac{1}{\Gamma(M)}\left[\frac{M}{R_0}\right]^M e^{\frac{MR}{R_0}} R^{-1+M} \quad (5)$$

where R_0 is the average pore radius and *M* is the shape parameter in the software. The shape parameter *M* is expressed by σ, the normalized dispersion normalized by average size, as follows (Rigaku Corporation 2006):

$$\sigma = \frac{\sqrt{\delta R^2}}{R_0} x100 = \frac{1}{\sqrt{M}} x100 \quad (6)$$

The pore size of HT1 and HT2 charcoals was also analyzed by N_2 adsorption at 77 K by a NOVA 2000 (Quantachrome Instruments, USA). The pore size was determined by the Barret-Joyner-Halenda (BJH) models (Barrett *et al*. 1951). In the case, surface area using Brunauer-Emmett-Teller (BET) equation (Brunauer *et al*. 1938) and adsorption isotherm in HT2 charcoals prepared by slow- and fast heat treatment were determined from N_2 adsorption at 77 K by a TriStar II 3020 (Micromeretics Instrument Corporation, USA).

A Raman spectroscopy (Renishaw inVia, England) equipped with an air-cooled CCD detector was used to analyze the carbon microstructure of the charcoals. An argon laser (514.5 nm) was adopted as an excitation source. The laser was focused to approximately 1 μm in diameter at a power of less than 1 mW on the charcoal surface in order to prevent irreversible thermal degradation. Spectra were measured in the 1,100-1,800 cm^{-1} range. Six 10-second accumulations gave adequate signal-to-noise ratio of the spectra. The wave number was calibrated using the 520 cm^{-1} line of a silicon wafer. Spectral processing was performed using WiRE 2 software. The crystallite size or coherence length (L_a) was determined from Raman peak data by an empirical formula developed by Tuinstra and Koening (1970):

$$L_a = \frac{(43.5\,\text{Å})}{I_d / I_g} \quad (7)$$

Proximate and Ultimate Analysis

Proximate analysis, including moisture, ash content, and volatile matter, were determined by ASTM D 2867-70, D 2866-70, and D 1762-64, respectively (1970; 1977). The fixed carbon content was obtained by difference. Ultimate analyzes was carried out by Perkin Elmer elemental analyzer 2400. The oxygen content was obtained by difference. The proximate and ultimate analyses were conducted on oil palm shell, HT1, and HT2 charcoals.

Results and Discussion

Pore Size Distribution

Fig. 2 shows an example of pore distribution analysis of a SAXS profile of HT2 charcoal by NANO-Solver, which was calculated by a curve fitting method where a simulated curve was to be fitted to a SAXS profile from scattering. In the SAXS profile, the scattering intensity in the low and high degree regions of 2θ attributed to inter- and intraparticle disorder, corresponding to meso- and micropore, respectively. The curve fitting analysis showed that the dominant pore structures of HT2 charcoal were micropores.

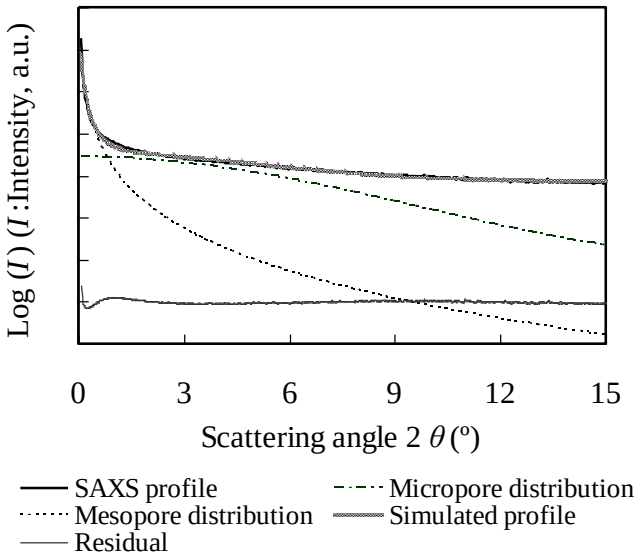

Figure 2. Analysis o pore distribution using NANO-Solver from a SAXS profile of HT2 charcoal which shows meso- and micropores in low and high degree region of 2. Micropore has the internal diameter less than 2 nm. Mesopore is that between 2 and 50 nm. The meaning of HT2 charcoal is referred to that in Table 1.

Table 2. BET Surface area and pore diameter analyzed by BJH model and by SAXS of HT1 and HT2 charcoals.

Charcoal	BET surface area (m^2/g)	BJH pore diameter (nm)	SAXS				
			Diameter of pore I (nm)	Vol. (%)	Diameter of pore II (nm)	Vol. (%)	Avr. Pore diameter (nm)
HT1	2.302	5.148	0.376	94.5	87.47	5.5	5.140
HT2	28.915	4.533	0.917	90.1	41.84	9.9	4.959

Note: The meaning of HT1 and HT2 is referred to that in Table 1. Pore I and II are referred to that in Fig. 2.

Table 2 lists the pore distribution, the volume fraction of pore and the average pore diameter of HT1 and HT2 charcoals measured by BJH method and analyzed by SAXS. The average pore diameter of HT1 and HT2 charcoals showed a minor difference and good agreement with that calculated by BJH method using N_2 adsorption analysis at 77 K (Barrett et al. 1951). On the other hand, wider distribution of mesopores was found in both HT1 and HT2 charcoals.

The size distribution of micropore in HT1 and HT2 charcoals are shown in Fig. 3. The average micropore size in HT1 charcoal was 0.376 nm which was smaller than that of 0.5 nm in the pine wood charcoal heat treated at 347ºC reported by Paris *et al*. (2005). The micropores were formed in HT1 charcoal when gas and tars evoluted up to 300ºC (Rodriguez-Reinoso and Molina-Sabio M 1992). In the case HT2 charcoal, the slope of SAXS profile increased slightly, equivalent to the greater diameter in the pores of 0.917 nm, which was greater than that of HT1 charcoal. The wider pore diameter with smaller distributions in HT2 charcoal was indicated by the slight increase in the SAXS signals. The heat treatments at 300ºC and followed by re-carbonization at 600ºC on HT2 charcoal released pyrolysis products which may influence on widening micropores already existed in the material. The micropore distribution of HT2 charcoal was smaller than that of HT1 charcoal, meaning that the widening of micropore might be occurred by connecting bigger pores leading to a certain pore size.

Figure 4a and c show the size distribution of micropore in HT1 charcoals in slow- and fast heating treatments. In slow heating treatment with additional $ZnCl_2$, lower scattering intensity of reaction time 120 and 180 min indicates lower porosity of the samples than that of 60 min. It is suggested that a prolonged reaction time from 60 min to 120 and 180 min caused the conversion of some micropore into wider pore sizes which reduced the porosity of the sample. The prolonged reaction time from 60 min to 120 min and 180 min also increased the diameter of micropore from 0.347 to 0.842 and 0.511 nm. In case of fast heating treatment, HT1 charcoals treated at different heating rates showed quite a similar scattering intensity which exhibited downward-convex profiles corresponding to a wide size distribution. The scattering intensity profiles of HT1 charcoals in fast heating treatment were lower than that in

slow heating treatment indicates lower porosity of the samples than that of HT1 charcoals in slow heating treatment.

Figure 4b and d show the size distribution of micropore in HT2 charcoals in slow- and fast heating treatments. In slow heating treatment, highest scattering intensity of reaction time 120 min and 180 min indicates higher porosity in the samples than that of 60 min. Heat treatment at 300ºC and then at 600ºC in the preparation HT2 charcoal may increase the release of volatile matters, resulting in widening micropore in the charcoal. Subsequent heat treatment at 700ºC for 120 and 180 min with additional $ZnCl_2$ enhanced the pores and created new micropore, which showed good agreement with the previous study (Lua *et al*. 2006) that reported the optimum temperature of carbonization at 600ºC for preparation of activated carbon. In the case of fast heating treatment, similar with previous discussion, the scattering intensity of samples was almost identical. The scattering intensity of HT2 charcoals in fast heating treatment was remarkable lower than that in slow heating treatment. However, fast heating treatment in a pulse current apparatus formed high distribution of homogeneous narrow micropore around 0.15-0.28 nm for HT1 charcoals and around 0.1 for HT2 charcoals which were different with an earlier investigation which reported that the fast heating produced macroporous carbon (Kurosaki *et al*. 2007).

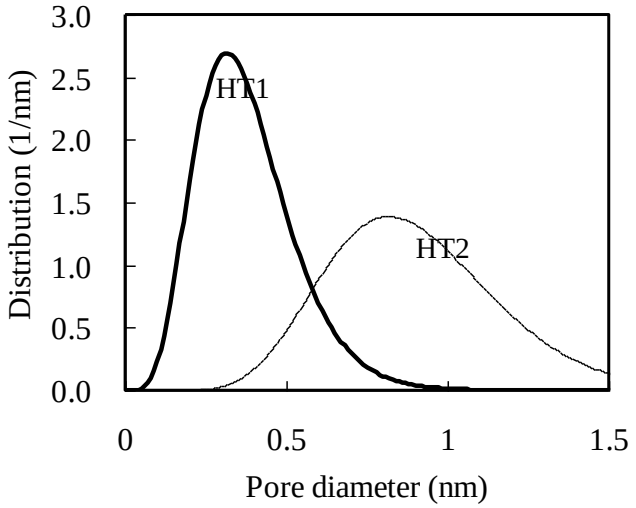

Fig. 3. Size distributions of micropores in HT1 and HT2 charcoals. The meaning of HT1 and HT2 is referred to that in Table 1.

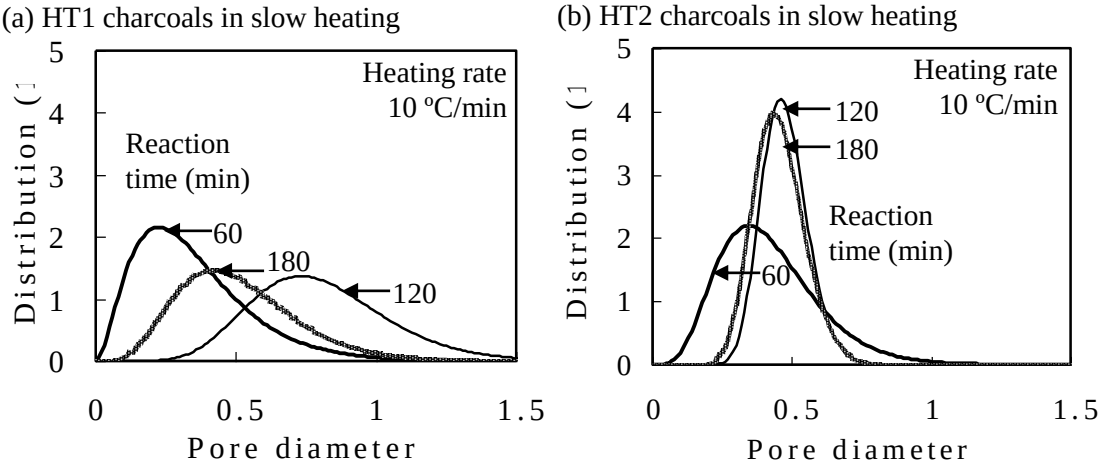

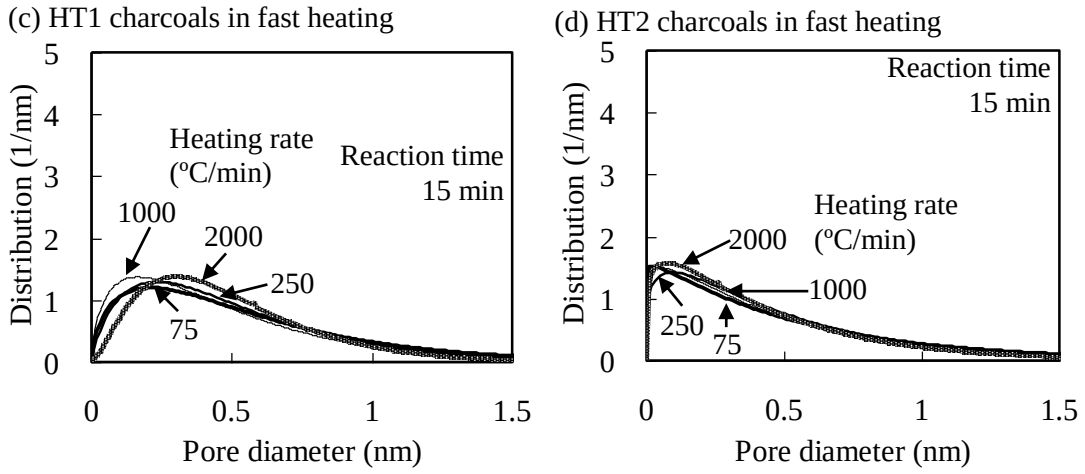

Figure 4. Size distributions of micropores in **a** HT1 and **b** HT2 charcoals heat-treated at 700ºC with heating rate 10ºC/min at different reaction times in slow heat treatment, in **c** HT1 and **d** HT2 chars heat-treated at 700ºC for 15 min at different heating rates in fast heating treatment. The meaning of HT1 and HT2 is referred to that in Table 1.

Surface Area

Surface area and adsorption isotherm were determined on HT2 charcoals in slow- and fast heating treatments due to the much different characteristics of micropore distribution. Figure 5a shows BET surface area of HT2 charcoals in slow heating treatment with additional $ZnCl_2$ in relationship to reaction time. HT2 charcoals prepared with reaction time 120 min and 180 min exhibited comparable BET surface area to the charcoal prepared with reaction time 60 min. The increasing porosity of HT2 charcoals in slow heating treatment due to the increasing reaction time from 60 min to 120 min and 180 min as shown by SAXS analysis was unable to be confirmed by gas adsorption analysis. A possible explanation is the closed porosity occurred in the charcoals prepared with reaction time 120 min and 180 min, which is not accessible for gas adsorption analysis.

Figure 5b shows BET surface area of HT2 charcoals in fast heating treatment in relationship to a heating rate. BET surface area of HT2 charcoals slightly increased with the increase of heating rate from 75 to 250ºC/min. Both BET surface area of HT2 charcoals prepared with heating rate 75 and 250ºC/min were comparable to HT2 charcoals in slow heating treatment. However, the increase of heating rate from 250 to 1000 and 2000ºC/min abruptly decreased BET surface area of HT2 charcoals with the value only 6.2 and 1.3 m^2/g, respectively. Fast heating may cause the surface of carbonized wood melted during the heat treatment with the rate of thousand degrees per minute (Diebold and Bridgwater 1997) which close or block the micropore which become inaccessible for gas adsorption analysis.

Figure 6a and b show the adsorption isotherm of HT2 charcoals in slow- and fast heating treatment. The shape of adsorption isotherms suggested that these charcoals exhibited Type I adsorption isotherms (Marsh and Rodriguez-Reinoso 2006) which containing microporosity only. Type I adsorption isotherm are typical of microporous solids in that micropore filling occurs significantly at relatively low partial pressure of < 0.1 P/P_o.[10]. HT2 charcoals in fast heating treatment prepared with reaction time 1000 and 2000ºC/min showed a low adsorption isotherm.

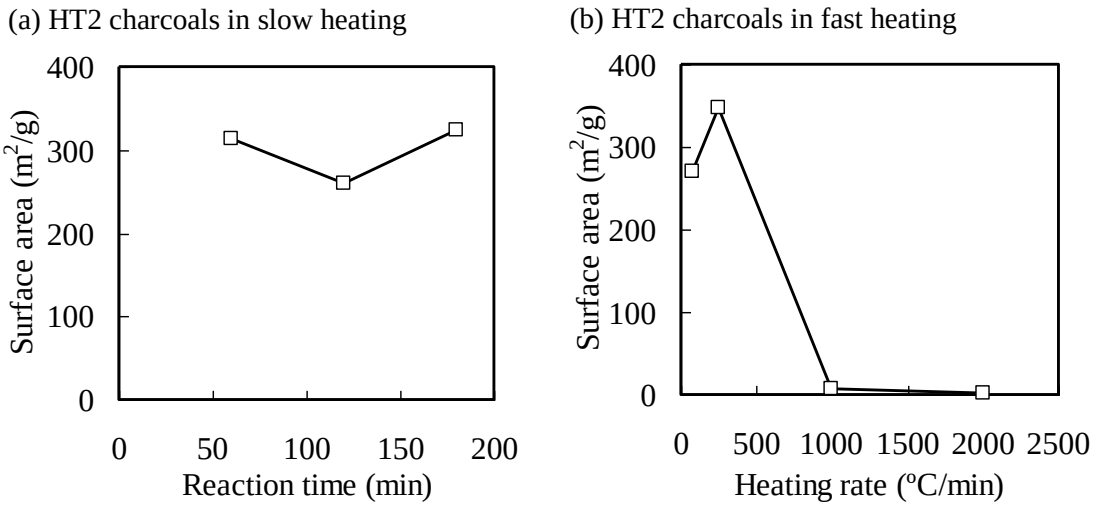

Figure 5. BET surface area of HT2 charcoals in **a** slow- and **b** fast heating treatment. The meaning of HT2 is referred to that in Table 1.

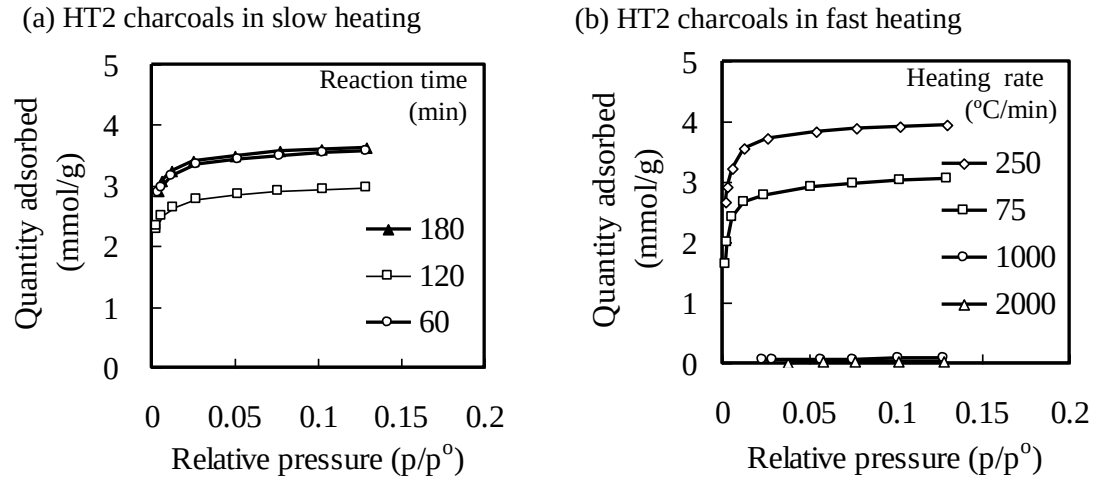

Figure 6. Adsorption isotherm of HT2 charcoals prepared by **a** slow- and **b** fast heating treatment. The meaning of HT2 is referred to that in Table 1.

Microstructural Change with Heat Treatments

Figure 7 shows the Raman spectra of HT1 and HT2 charcoals which exhibited D-band and G-band attributed to graphitic sp^2-bonded carbon. D-band is usually associated with the disordered structure of turbostratic carbon and G-band corresponds to the crystalline vibration (Ishimaru *et al.* 2007); Paris 2005). HT1 charcoal prepared from a heat treatment at 300ºC exhibited broad D-band and G-band with full width at half maximum (FWHM) of 279 and 125 cm^{-1}, respectively, corresponding to a typical of least ordered carbon material. The appearing of D-band and G-band on HT1 charcoal showed the aromatization occurred at heat treatment at 300ºC. HT2 charcoal prepared from a heat treatment at 300ºC and followed by re-carbonization at 600ºC showed narrowing D-band and G-band with FWHM of 206 and 82 cm^{-1} at positions shifted to 1362 and 1601, indicating the ordering of microstructure in the charcoal which was agreed with a previous study (Rodriguez-Reinoso and Molina-Sabio 1992) that reported the charcoal structure was consolidated at temperature range between 770-1120K. However the FWHM of D-band of HT2 charcoal was broader than that of carbonized wood reported previously (Yamauchi and Kurimoto Y 2003).

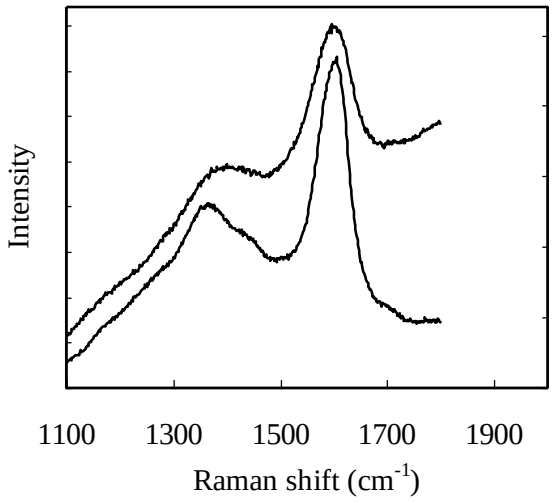

Figure 7. Raman spectra of HT1 and HT2 charcoals. The meaning of HT1 and HT2 is referred to that in Table 1.

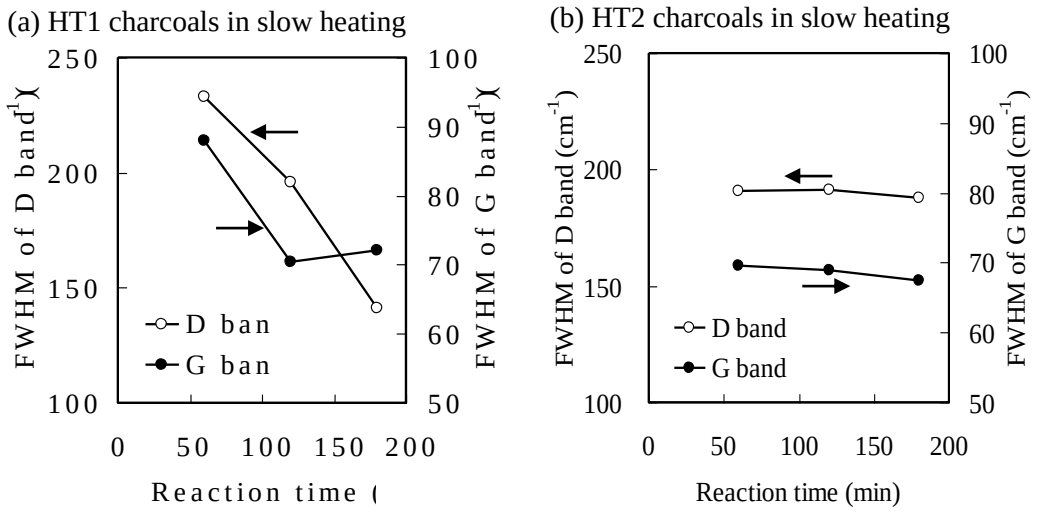

Figure 8. FWHM of D-band and G-band of **a** HT1 and **b** HT2 charcoals in slow heating treatment in relationship to reaction time. The meaning of HT1 and HT2 is referred to that in Table 1.

Effect of Slow Heating Treatment on Microstructural Change

Figure 8a and b show the plot of D-band and G-band width (FWHM) of HT1 and HT2 charcoals in slow heating treatment in relationship to reaction times. The FWHM of D-band and G-band of HT1 charcoals decreased with the increasing reaction time. The narrowing of band width suggests the structural arrangement or the ordering carbon element with the increase in reaction time (Yamauchi and Kurimoto Y 2003). The D-band and G-band of HT2 charcoals slow-heat-treated were narrower than that of HT1 charcoals slow-heat-treated for the reaction time of 60 and 120 min. It is suggested that re-carbonization at 600ºC, as second step of the slow heat treatment on HT2 charcoals contributed to the ordering microstructure. Prolonged reaction time of 180 min influenced significantly on the ordering of microstructure HT1 charcoal slow-heat-treated.

Effect of Fast Heating Treatment on Microstructural Change

The FWHM of D-band and G-band of HT1 and HT2 charcoals in fast-heating treatment in relationship to heating rates are shown in Fig. 9a and b. The FWHM of D-band and G-band of both HT1 and HT2 charcoals in fast heating

treatment became broader with the increasing heating rate. Meanwhile, HT1 charcoals fast-heat-treated showed broader D-band which indicated strong defects occurred compared with fast-heat-treated HT2 charcoals. As discussed on previously, fast heating treatment promotes the simultaneous chemical reactions including fragmentation and re-polymeration leading to a large formation of volatile matter (Kurosaki *et al*. 2003). HT1 charcoals released more intensively volatile matters during the fast heating treatment than that of HT2 charcoals. It is suggested that the fast volatilization contributed to more defects occurrence in the microstructure of HT1 charcoals. The defects in the microstructure of the charcoals intensively occurred with the increase of heating rate as shown by the broadening of the FWHM of D band. Therefore the fast heat treatments produced charcoal with lesser microstructural ordering than that of the slow heat treatments.

Figure 10a and b show the coherence length (L_a) of HT1 and HT2 charcoals in slow- and fast heating treatments, respectively. The L_a was reported to dependence on temperature with a decreasing trend with the increase of temperature (Paris 2005). In this study, L_a was insensitive to the increasing reaction time in slow heating treatments, as shown in Fig 10a and to the increasing heating rate in fast heating treatments, as shown in Fig 10b. HT1 and HT2 charcoals slow heat-treated at 10ºC/min up to 700ºC possessed higher L_a than that of HT1 and HT2 charcoals fast- heat-treated. It is suggested that the different chemical reaction occurred during the volatilization in the slow- and fast heating treatment as discussed previously may affect the growth of turbostratic crystallites

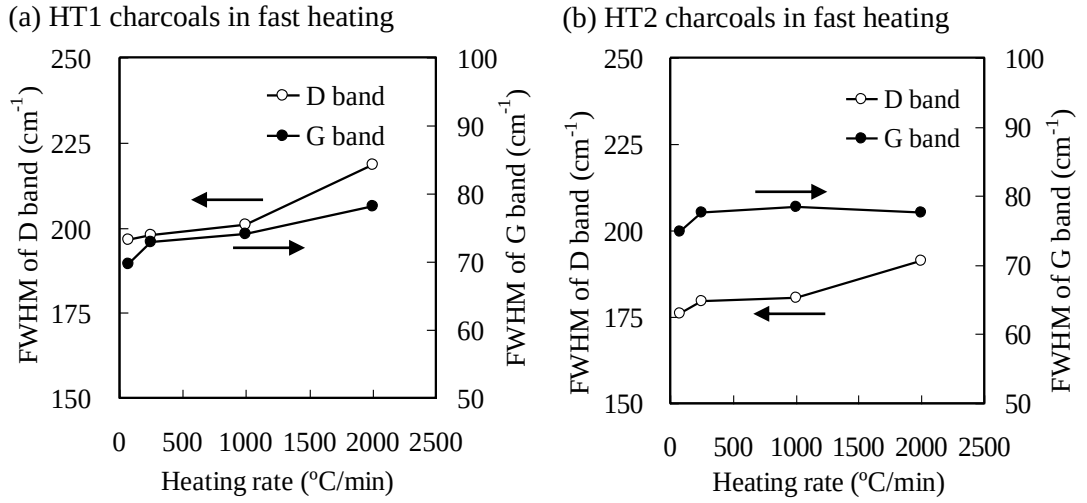

Figure 9. FWHM of D-band and G-band of **a** HT1 and **b** HT2 charcoals in fast heating treatment with the function of heating rate. The meaning of HT1 and HT2 is referred to that in Table 1.

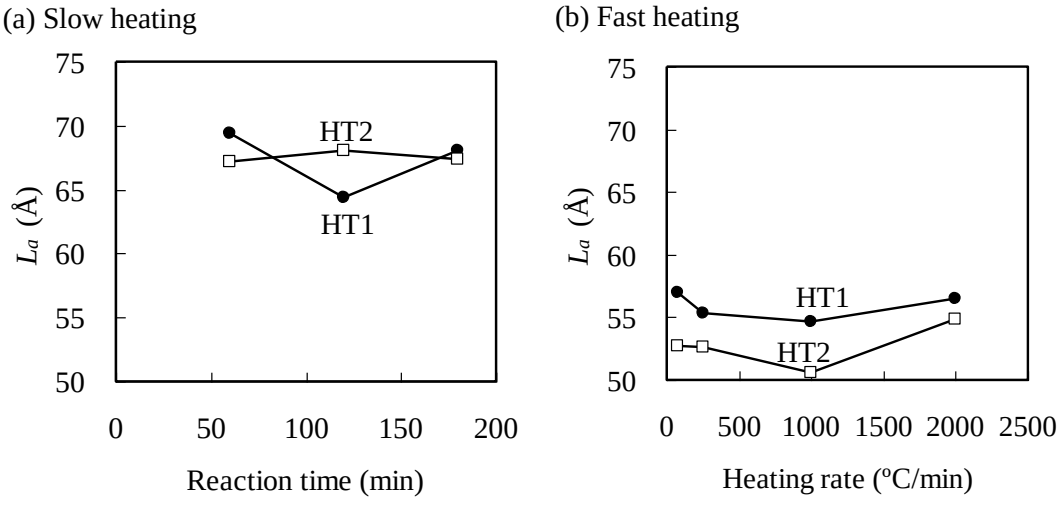

Figure 10. Coherence Length (L_a) of HT1 and HT2 charcoals **a** in slow- and **b** fast heat-treatment. *Filled circles*, HT1 chars; *empty squares*, HT2 chars. The meaning of HT1 and HT2 is referred to that in Table 1.

Conclusions

A slow heating treatment up to 700ºC on HT1 charcoal with the increasing reaction time for 120 and 180 min lead to the widening of micropore diameter without the opening new micropores indicating a reducing porosity and with the ordering microstructure comparing with those in HT1 charcoal with the reaction time for 60 min. Fast heating treatment on HT1 charcoal created micropore with narrower diameter and wider size distribution, but with lesser porosity and the disordering microstructure comparing with those in HT1 charcoal slow heat treated. In fast heating treatment on HT1 charcoal, the increase of heating rate produced charcoal with the decreasing micropore diameter and quite similar micropore size distribution, but with the disordering microstructure.

Re-carbonization at 600ºC in the preparation of HT2 charcoal contributed on the opening the new micropore with average diameter around 0.452-0.474 nm and on the ordering microstructure in the charcoals after the slow heat treatment up to 700ºC for 120 and 180 min. But some parts of the micropore in HT2 charcoal slow heat treated were inaccessible for N_2 gas. The increase of heating rate in fast heating treatment of HT2 charcoal was unchanged the distribution of micropore size and affected on the disordering microstructure. But BET surface area of HT2 charcoals slightly increased with the increase of heating rate from 75 to 250ºC/min then decreased with the increase of heating rate to 1000 and 2000ºC/min.

References

American Society for Testing and Materials. 1970. ASTM D 2867-70 Moisture in Activated Carbon.

American Society for Testing and Materials. 1970. ASTM D 2866-70 Total Ash Content of Activated Carbon.

American Society for Testing and Materials. 1977. ASTM D 1762-64 (Reapproved 1977) Chemical Analysis of Wood Charcoal.

Barrett, E.P.; L.G. Joyner; and P.P. Halenda. 1951. The Determination of Pore Volume and Area Distributions in Porous Substances I: Computational from Nitrogen Isotherms. J Am Chem Soc 73: 373-380.

Brunauer, S.; P.H. Emmett; and E. Teller. 1938. Adsorption of Gases in Multimolecular Layers. J Am Chem Soc 0: 309-319.

Demirbas, A. 2001. Carbonization Ranking of Selected Biomass for Charcoal, Liquid and Gaseous Products. Eng Convers and Management 42: 1229-1238.

Diebold, J.P. and A.V. Bridgwater. 1997. In: Bridgwater AV, Boocock DGB (Eds.) Development in Thermochemical Biomass Conversion, Vol. 1, Blackie Academic & Professional.

Fujisawa, M., T. Hata; P. Bronsveld; V. Castro; F. Tanaka; H. Kikuchi; T. Furuno; and Y. Imamura. 2004. SiC/C Composites Prepared from Wood-based Carbons by Pulse Current Sintering with SiO_2: Electrical and Thermal Properties. J Eur Ceram Soc 24: 3575-3580.

Greil, P. 2001. Biomorphous Ceramics from Lignocellulosics. J Eur Cer Soc 21: 105-118.

Ishimaru, K.; T. Hata; P. Bronsveld; and Y. Imamura Y. 2007. Microsectioning Study of Carbonized Wood after Cell Wall Sectioning. J Mater Sci 42: 2662-2668.

KE Hattula T.; U.M. Mrouch; and T. Luoma. 2001. Use of Liquid Smoke Flavouring as an Alternative to Traditional Flue Gas Smoking of Rainbow Trout Fillets (*Onchorhynchus mykiss*). Lebensm.-Wiss U-Technol 34: 521-525.

Kurosaki, F.; K. Ishimaru; T. Hata; P. Bronsveld; E. Kobayashi; and Y. Imamura. 2003. Microstructure of Wood Charcoal Prepared by Flash Heating. Carbon 41: 3057-3062.

Kurosaki, F.; H. Koyanaka; T. Hata; and Y. Imamura. 2007. Macroporus Carbon Prepared by Flash Heating of Sawdust. Carbon 45: 668-689.

Lua, A.C.; F.Y. Lau; and J. Guo. 2006. Influence of Pyrolysis Conditions on Pore Development of Oil-palm-shell Activated Carbons. J Anal Appl Pyrolysis 76: 96-102.

Mackay, D.M. and P.V. Roberts. 1981) The influence of pyrolysis conditions on yield and microporosity of lignocellulosic charcoals. Carbon 20: 95-104.

Marsh, H. and F. Rodriguez-Reinoso. 2006. Activated Carbon. Elsevier Ltd.

Paris, O.; C. Zollfrank; and G.A. Zickler. 2005. Decomposition and Carbonization of Wood Biopolymers-a Microstructural Study of Softwood Pyrolysis. Carbon 43: 53-66.

Pastor-Villegas, J.; C. Valenzuela-Calahorro; A. Bernalte-Garcia; and V. Gomez-Serrano. 1993. Characterization Study of Charcoal and Activated Carbon Prepared from Raw and Extracted Rockrose. Carbon 31: 1061-1069.

Rigaku Corporation. 2006. Cat. No. 9289H901/902 NANO-Solver (Ver3.4): Particle-/pore-size analysis software instruction manual. Manual No. ME13266A06, Sixth Edition. Japan.

Rodriguez-Reinoso, F. and M. Molina-Sabio. 1992. Activated Carbon from Lignocellulosic Materials by Chemical and/or Physical Activation: An Overview. Carbon 30: 1111-1118.

Tuinstra, F. and J.L. Koenig. 1970. Raman Spectrum of Graphite. J Chem Phys 53: 1126-1230.

Sulistyo, J.; T. Hata; H. Kitagawa; P. Bronsveld; M. Fujisawa; K. Hashimoto; and Y. Imamura. 2010. Electrical and Thermal Conductivities of Porous SiC/SiO_2/C Composites with Different Morphology from Carbonized Wood. J Mater Sci 45: 1107-1116.

Vyshnyakova, K.; G. Yushin; L. Pereselentseva; and Y. Gogotsi. 2006. Formation of Porous SiC Ceramics by Pyrolysis of Wood Impregnated with Silica. Intl J Appl Ceram Technol 3: 485-490.

Yamauchi, S. and Y. Kurimoto. 2003. Raman Spectroscopy Study on Pyrolyzed Wood and Bark of Japanese cedar: Temperature Dependence of Raman Parameters. J Wood Sci 49: 235-240.

Joko Sulistyo, Purnomo Darmadji and Sri Nugroho Marsoem
Faculty of Forestry, Universitas Gadjah Mada, Indonesia
Jl. Agro No. 1. Bulaksumur, Yogyakarta, Indonesia 55281
Tel : 62-274-6491428
Fax : 62-274-550541
E-mail : jsulistyo@ugm.ac.id

Toshimitsu Hata and Yuji Imamura (former)
Laboratory of Innovative Humano-habitability
Research Institute for Sustainable Humanosphere,
Kyoto University
Uji Campus, Gokasho, Uji, Kyoto 611-0011, Japan.
Tel. : +81-774-38-3601
Fax. : +81-774-38-3600
E-mail : hata@rish.kyoto-u.ac.jp